Journal of Molecular Structure 987 (2011) 126–131

Contents lists available at ScienceDirect

Journal of Molecular Structure

journal homepage: www.elsevier.com/locate/molstruc

Syntheses, crystal structure, and luminescence properties of three new Cd(II) polymers based on different conformational carboxylates

Jian-Qiang Liu [a,*], Zhen-Bin Jia [a], Yao-Yu Wang [b]

[a] *Guangdong Medical College, School of Pharmacy, Dongguan 523808, PR China*
[b] *Key Laboratory of Synthetic and Natural Functional Molecule Chemistry of the Ministry of Education, Shaanxi Key Laboratory of Physico-Inorganic Chemistry, Department of Chemistry, Northwest University, Xi'an 710069, PR China*

ARTICLE INFO

Article history:
Received 1 November 2010
Received in revised form 6 December 2010
Accepted 6 December 2010
Available online 13 December 2010

Keywords:
Crystal structure
Cd(II) complex
Self-assembly
Luminescent property

ABSTRACT

Three new coordination polymers, namely, $\{[Cd_3(L_1)_2(IP)_2(H_2O)_4]\}_n$ (**1**), $\{[Cd_2(L_2)_2(IP)_2]\cdot(CH_3OH)(DMF)\}_n$ (**2**) and $[Cd(L_3)(IP)]_n$ (**3**) (H_3L_1 = benzene-1,2,4-tricarboxylic acid, H_2L_2 = 2,2-bis(4-carboxyphenyl)hexafluoropropane, H_2L_3 = 1,3-phenylenediacetic acid and IP = 1H-imidazo[4,5-f][1,10]-phenanthroline), were prepared *via* self-assembly of pharmaceutical agent IP with cadmium sulfate in the presence of the different backbones of carboxylate linkers under mild conditions. All the polymers possess 2D structural motifs. The rigid tricarboxylate ligand links the metal centers to form a tetranuclear core in **1**. In **2**, the 2D network with trinuclear cores is further extended into 3D supramolecular arrays through aromatic stacking interactions. Interestingly, IP ligand acts in a tridentate mode *via* the two N atoms of pyridyl rings and the third N atom of imidazole ring and connects metal atoms into 1D zigzag chain in **3**. The structural analysis reveals that the backbones of carboxylates have critical effect on the construction of the complexes. Solid-state luminescent spectra of the Cd(II) complexes indicate intense fluorescent emissions.

1. Introduction

The flourishing realm of crystal engineering has provided a sound junction between aesthetics of crystalline architectures and their potential functions [1–3], of which the ultimate destination is to successfully achieve the target materials with tailored structures and/or physicochemical properties. In a general way, the diversity in the networks of such materials greatly depends on the selection of metal centers with kinds of coordination preference and organic spacers with modifiable backbones and connectivity information [4–10]. The selection of the organic ligand to be bonded to the metal atom plays a pivotal role in the resulting structure of MOF. For example, the bent configuration or angular disposition of coordinating sites of the ligand could generate to a grid motif [4b]. Nevertheless, it is still a great challenge to predict the exact structures and compositions of compounds by careful selection of organic ligands[11–19].

Recently, a comprehensive analysis of the predicted diversity of coordination polymers with IP has been carried out by us [20]. These results reveal that the backbones of carboxylates and natures of metal ions are reliable to obtain unusual frameworks with particular properties. As a continuation of this attractive project, we employ other types of backbones of carboxylates and explore their effects on metal–organic frameworks. In this context, we will describe three new Cd(II) coordination polymers with different structural characters. The thermal stabilities and solid-state properties for these crystalline materials will also be investigated.

2. Experimental abbreviations

H_3L_1 = benzene-1,2,4-tricarboxylic acid, H_2L_2 = 2,2-bis(4-carboxyphenyl)hexafluoropropane, H_2L_3 = 1,3-phenylenediacetic acid and IP = 1H-imidazo[4,5-f][1,10]-phenanthroline.

2.1. Materials and physical measurements

All the reagents were purchased from commercial sources and used as received. FT-IR spectra (KBr pellets) were taken on a FT-IR 170SX (Nicolet) spectrometer. The luminescent spectra of the solid samples were acquired at ambient temperature by using a JOBIN YVON/HORIBA SPEX Fluorolog t3 system (slit: 0.2 nm). Elemental analyses were performed on a Perkin–Elmer 240C analyzer. TG analyses were carried out with a Mettler-Toledo TA 50 in dry nitrogen (60 mL min^{-1}) at a heating rate of 5 °C min^{-1}. X-ray power diffraction (XRPD) data were recorded on a Rigaku RU200 diffractometer at 60 kV, 300 mA for Cu Kα radiation

---

[*] Corresponding author.
E-mail address: deposit@ccdc.cam.ac.uk (J.-Q. Liu).

0022-2860/$ - see front matter © 2010 Elsevier B.V. All rights reserved.
doi:10.1016/j.molstruc.2010.12.006

(λ = 1.5406 Å), with a scan speed of 2 °C/min and a step size of 0.02° in 2θ.

3. X-ray crystallography

Single crystal X-ray diffraction analyses of the three compounds were carried out on a *Bruker SMART APEX II CCD* diffractometer equipped with a graphite monochromated Mo Kα radiation (λ = 0.71073 Å) by using ϕ/ω scan technique at room temperature. The intensities were corrected for Lorentz and polarization effects as well as for empirical absorption based on multi-scan techniques; all structures were solved by direct methods and refined by full-matrix least-squares fitting on F^2 by *SHELX-97* [21]. Absorption corrections were applied by using multi-scan program *SADABS* [22].The hydrogen atoms of organic ligands were placed in calculated positions and refined using a riding on attached atoms with isotropic thermal parameters 1.2 times those of their carrier atoms. The water hydrogen atoms were located from difference maps and refined with isotropic thermal parameters 1.5 times those of their carrier atoms. Table 1 shows crystallographic data of **1**–**3**. Selected bond distances and bond angles are listed in Table 2.

Table 2
Selected bond distances (Å) and angles (°).

*Complex **1***			
Cd1–O2	2.224(4)	Cd1–O3	2.335(5)
Cd1–O4	2.277(5)	Cd1–N1	2.388(4)
Cd1–N2	2.354(5)	Cd1–O5#2	2.333(4)
Cd2–O1	2.336(4)	Cd2–O6	2.401(4)
Cd2–O7#1	2.175(4)	Cd2–O1#3	2.336(4)
Cd2–O6#3	2.401(4)	Cd2–O7#1	2.175(4)
O2–Cd1–O4	113.81(18)	O6–Cd2–O7#1	80.22(15)
O2–Cd1–N1	87.66(16)	O2–Cd1–N2	157.48(16)
O2–Cd1–O5#2	84.74(15)	O3–Cd1–O4	89.82(19)
O3–Cd1–O5#2	177.35(15)	O4–Cd1–N1	158.50(18)
#1: $x, -1+y, z$; #2: $1+x, y, z$; #3: $1-x, 1-y, -z$			
*Complex **2***			
Cd1–O1	2.182(3)	Cd1–O5	2.197(4)
Cd1–N1	2.308(4)	Cd1–N2	2.349(4)
Cd1–O3#1	2.463(4)	Cd1–O4#1	2.329(3)
Cd2–O2	2.267(3)	Cd2–O6	2.272(4)
Cd2–O4#1	2.318(3)	Cd2–O2#2	2.267(3)
Cd2–O6#2	2.272(4)	Cd2–O4#1	2.318(3)
O1–Cd1–O5	97.03(15)	O6–Cd2–O6#2	180.00
O1–Cd1–N1	114.49(15)	O4–Cd2–O6	86.15(13)
O1–Cd1–O3#1	146.49(13)	O4–Cd2–O6#2	86.15(13
O1–Cd1–O4#1	92.72(13)	O4–Cd2–O4#1	180.00
#1: $x, y, -1+z$; #2: $1/2-x, 1/2-y, 1-z$			
*Complex **3***			
Cd1–O1	2.511(7)	Cd1–O2	2.395(7)
Cd1–N1	2.394(7)	Cd1–N2	2.369(7)
Cd1–O3#1	2.451(8)	Cd1–O4#1	2.363(8)
Cd1–N3#2	2.377(8)		
O–Cd1–O2	52.9(2)	O1–Cd1–N1	77.1(2)
O1–Cd1–N2	94.1(2)	O1–Cd1–O3#1	167.9(3)
O1–Cd1–O4#1	133.4(2)	N1–Cd1–N3#2	146.5(3)
O2–Cd1–N1	96.0(2)	O2–Cd1–N2	146.8(2)
O2–Cd1–O3#1	125.9(3)	O2–Cd1–O4#1	85.5(2)
#1: $1-x, 1/2+y, 5/2-z$; #2: $x, 3/2-y, 1/2+z$			

4. Synthesis of the complexes

4.1. $\{[Cd_3(L_1)_2(IP)_2(H_2O)_4]\}_n$ (**1**)

Compound **1** was prepared as follows: a mixture of $CdSO_4H_2O$ (0.027 g, 0.11 mmol), IP (0.022 g, 0.1 mmol), H_3L_1 (0.021, 0.1 mmol), NaOH (0.1 mmol), CH_3OH (2 mL) and DMF (1 mL) and deionised water (8 mL) was stirred for 20 min in air, then transferred and sealed in a 25-mL Teflon reactor, which was heated at 150 °C for 72 h. The solution was then cooled to room temperature at rate of 5 °C h^{-1}, to yield pale yellow crystalline product of **1** in 45% yield based on Cd. $C_{22}H_{15}Cd_{1.50}N_4O_8$ (**1**) (1544.28) Calcd: C, 41.81; H, 2.39; N, 8.87. Found C, 41.67; H, 2.42; N, 8.85. **IR** (KBr, cm^{-1}): 3569(m), 2291(w), 1512(s), 1205(m), 648(s).

4.2. $\{[Cd_2(L_2)_2(IP)_2]\cdot(CH_3OH)(DMF)\}_n$ (**2**)

The synthesis procedure of **2** is similar to that for **1** except that H_3L_1 is replaced by H_2L_2. $C_{56.67}H_{42.67}Cd_2F_{12}N_{6.67}O_{12}$ (**2**) Calcd: C, 46.56; H, 2.94; N, 6.39. Found C, 46.60; H, 2.98; N, 6.51. **IR** (KBr, cm^{-1}): 3212(m), 2591(m),1569(s), 1288(m), 655(s).

4.3. $[Cd(L_3)(IP)]_n$ (**3**)

The synthesis procedure of **3** is similar to that for **1** except that H_3L_1 is replaced by H_2L_3. $C_{23}H_{16}CdN_4O_4$ (**3**) Calcd: C, 52.63; H, 3.07;

Table 1
Crystal data and structure refinement information for compounds **1**–**3**.

Compounds	**1**	**2**	**3**
Formula	$C_{22}H_{15}Cd_{1.50}N_4O_8$	$C_{56.67}H_{42.67}Cd_2F_{12}N_{6.67}O_{12}$	$C_{23}H_{16}CdN_4O_4$
Fw	631.98	1461.77	524.80
Temp. (K)	298(2)	298(2)	298(2)
Cryst system	Trinlinic	Monoclinic	Monoclinic
Space group	$P-1$	$C2/c$	$P2_1/c$
a (Å)	7.5213(12)	24.1063(17)	1.2116(13)
b (Å)	9.5403(15)	25.1877(18)	16.029(3)
c (Å)	15.238(2)	14.5654(10)	17.056(3)
α (°)	73.893(2)	90	90
β (°)	79.037(2)	101.0930(10)	98.882(2)
γ (°)	81.934(2)	90	90
V (Å^3)	1026.9(3)	8678.6(11)	1948.0(6)
Z	2	6	4
$F(0\,0\,0)$	622	4376	1048
D_c (g/cm^3)	2.044	1.678	1.789
GOF	0.875	1.089	0.965
Reflections collected	3599	7788	3479
Unique reflections	5121(R_{int} = 0.0225)	21,745(R_{int} = 0.0349)	9458 (R_{int} = 0.1021)
Final R indices	R_1 = 0.0398	R_1 = 0.0457	R_1 = 0.0769
($R^{\alpha}(I > 2\sigma(I))$	wR_2 = 0.1124	wR_2 = 0.1434	wR_2 = 0.2025
R indices	R_1 = 0.0557	R_1 = 0.0457	R_1 = 0.0904
(All data)	wR_2 = 0.1286	wR_2 = 0.1600	wR_2 = 0.2167

$^{a}R_1 = \sum||F_0| - |F_c||/\sum|F_0|$, $wR_2 = \{\sum[w(F_0^2 - F_c^2)^2]/\sum(F_0^2)^2\}^{1/2}$.

N, 10.68. Found C, 52.60; H, 3.12; N, 10.61. **IR** (KBr, cm^{-1}): 2028(m), 1618(s), 1216(m), 638(s).

5. Results and discussion

5.1. Crystal structure of $\{[Cd_3(L_1)_2(IP)_2(H_2O)_4]\}_n$ (1)

Single-crystal X-ray structural analysis reveals that the asymmetric unit of **1** contains one and a half Cd(II) atoms, one L_1 ligand, one IP and two coordination water molecules. Fig. 1a shows the view of the local coordination geometries around the Cd(II) atoms. The two Cd(II) atoms have different coordinative environments. As for Cd1, the axial positions are occupied by one oxygen atom from one bidentate carboxylate group and one oxygen atom from one coordinative water molecule, whereas two oxygen atoms from one coordinative water molecule and one bidentate carboxylate end and two nitrogen atoms from one chelating IP ligand are on the equatorial plane. The Cd2 has ideal octahedral coordination geometry. The axial positions are occupied by two oxygen atoms from two symmetric monodentate carboxylate groups, while the four oxygen atoms from carboxylate groups of two different L_1 ligands locate on the equatorial plane. The Cd–O bond distances range from 2.175(4) to 2.401(4) Å, and the Cd–N bond distances range from 2.354(5) to 2.388(5) Å. The three carboxylate groups exhibit two kinds of coordination modes (monodentate and bridging bidentate fashions). Based on these connection nodes, four Cd(II) ions are bridged by four μ_2–carboxylate ends to give tetranuclear units, which are further extended by monodentate carboxylate ends into 2D layers along the *ab* plane, as shown in Fig. 1b. From the [1 0 1] direction, nano-channels are directed by Cd ions and L_1 ligands (Fig. 1c and d). As presented in Fig. 1e, the Cd1 and Cd2 atoms are linked by $O_2C–C–CO_2$ groups of L_1 ligand to form the left- and right-handed helical chains running along the *c* axis with a pitch of 12.86 Å. In addition, the interplanar distance between pyridyl rings of IP ligands is *ca.* 3.86(5) Å, indicating the presence of weak π–π stacking interaction that further stabilizes the crystal structure (Fig. 1f).

5.2. Crystal structure of $\{[Cd_2(L_2)_2(IP)_2]\cdot(CH_3OH)(DMF)\}_n$ (**2**)

In the structure, there are two crystallographically unique Cd(II) atoms. The central Cd2 atom in each unit lies on an inversion centre and is coordinated by six oxygen atoms from separated L_2 ligands (Cd–O bond distances range from 2.267(3) to 2.318(3) Å), whereas the terminal Cd1 atom is coordinated by four oxygen atoms (Cd–O bond distances range from 2.182(4) to 2.463(4) Å) and two nitrogen atoms (Fig. 2a). Similar trinuclear $Cd_3(RCO_2)_6$ cluster has been reported, in which is assembled from Cd atom and flexible organic unit[4,23]. In the asymmetric unit, there are two types of $L_2(1)$ and $L_2(2)$ ligands. The $L_2(1)$ adopts $(k^1–k^1)–(k^1–k^1)–\mu_4$ fashion and links the tri-metallic core to form a 1D chain along the *c* direction, while $L_2(2)$ adopts $(k^1–k^1)–(k^2–\mu_2)–\mu_4$ mode and connects the trinuclear unit to shape another 1D chain along the *a* axis.

View from the *ac* plane reveals a (4, 4) topology structure (Fig. 2b). The space is occupied by the guest CH_3OH and DMF molecules. Each layer is slightly offset compared to adjacent layers (Fig. 2d). A striking feature of **2** is the alternating arrangement of three types of helices along *a* axis, which are formed by Cd2 and two types of $L_2(1)$ and $L_2(2)$ ligands (Fig. 2c). The strong aromatic stacking interaction of neighboring IP molecules is ca. 3.63(6) Å), which further extended the structure into 3D framework (Fig. 2e).

5.3. Crystal structure of $[Cd(L_3)(IP)]_n$ (**3**)

To further investigate the effect of assistant ligand on the framework, the angular backbone of organic ligand was deliberately employed. 1,3-Phenylenediacetic acid was introduced into the Cd-IP system. A new compound **3** was obtained. The structure of **3** has neutral sheet of $[Cd(L_3)(IP)]_n$. The Cd(II) ion is coordinated by four oxygen atoms from two carboxylate groups and three nitrogen atoms from two pyridine rings and one imidazole ring (Fig. 3a). The Cd(II) metal centers are connected to each other by L_3 with *syn–syn* fashion into a 1D helical chain (Fig. 3c). In **3**, IP adopts a μ_2-bridging mode, linking the adjacent metal ions into a zigzag chain (Fig. 3d). Ultimately, the whole structure displays a 2D framework. As shown in Fig. 3b. Each layer is slightly offset compared to adjacent layers (Fig. 3e and f).

5.4. Comparison of the structures of coordination polymers

As a matter of fact, the coordination frameworks of most complexes are not only influenced by metal ions, but also depend on the reliable coordinative sites of carboxylate ligands. In this work, we select three kinds of rigid/flexible carboxylic acid with H_3L_1, H_2L_2 and H_2L_3, and intend to explore their effects on the assembly

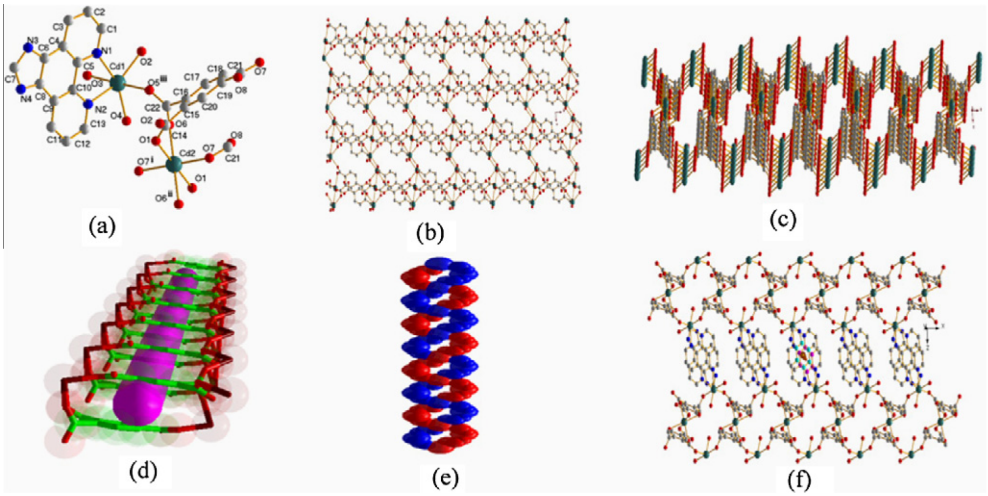

Fig. 1. (a) Stick representation of the coordination environments of the Cd(II) ions in **1** (i: $x, -1 + y, z$; ii: $1 + x, y, z$; ii: $1 - x, 1 - y, -z$). Hydrogen atoms have been omitted for clarity; (b) view of the 2D layer along *ab* plane; (c) the 2D layer long ac direction; (d) view of 1D nano-tube channels along *ac* plane; (e) Schematic view of the double helical chains; (f) the 3D supramolecular framework formed by aromatic stacking interactions.

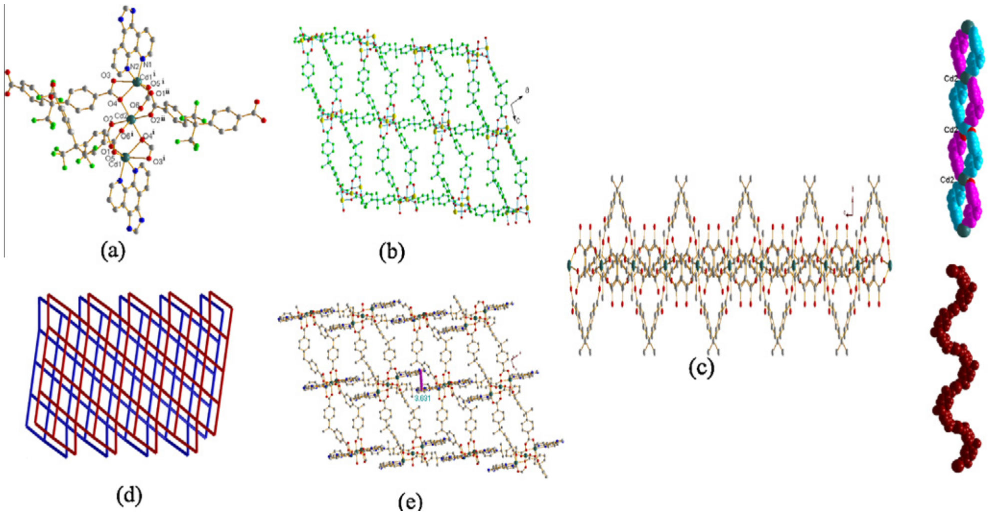

Fig. 2. (a) Stick representation of the coordination environments of the Cd(II) ions in **2** (i: $x, y, -1+z$; ii: $1/2-x, 1/2-y, 1-z$). Hydrogen atoms have been omitted for clarity; (b) perspective view of 2D layer in **2**; (c) three types of helical chains directed by Cd(2) ions and L_2 ligands; (d) view of the adjacent offset grid sheet; (e) 3D supramolecular net formed by strong aromatic stacking interactions.

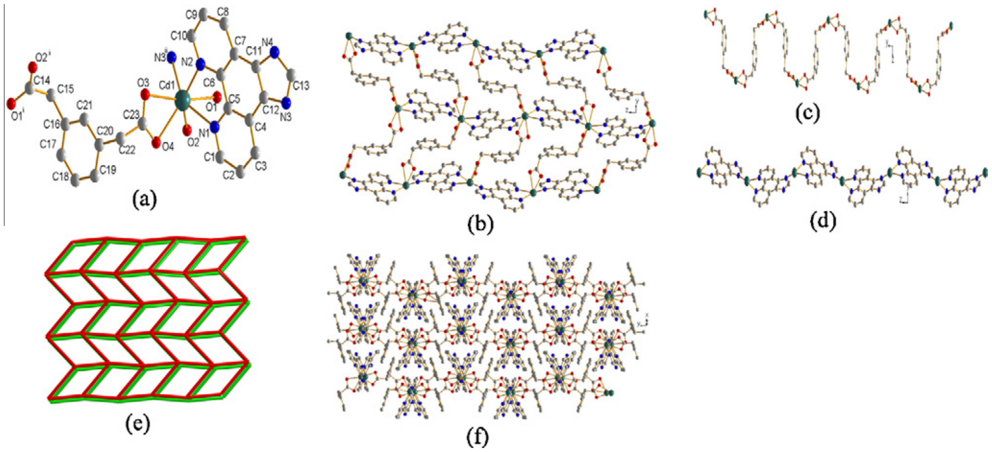

Fig. 3. (a) Stick representation of the coordination environment of the Cd(II) ion in **3**(i: $1-x, 1/2+y, 5/2-z$; ii: $x, 3/2-y, 1/2+z$); hydrogen atoms have been omitted for clarity; (b) perspective view of 2D layer in **3**; (c) view of 1D helical chain; (d) view of the 1D zigzag chain; (e) cross section of 3 viewed along ac plane; (f) the butterfly-like layers.

of the Cd-IP coordination system (see Scheme 1). In compound **1**, the small backbone makes it possible for L_1 to provide more chance to bind more metal ions and form polynuclear core. In addition, the formation of tetranuclear Cd(II) cores may reduce the coordinative chance of N atom from imidazole ring of IP to bond to metal atoms. As for compound **3**, the N atom from imidazole ring coordinates to metal atom. Finally, a new grid layer is shaped. The incorporation of the changeable backbone length between L_2 and L_3 determines the difference of the pitch of the helices and helical degree in **2** and **3**. Consequently, **2** features undulating Cd(II)/L_2 layer from three types of helical chains; in **3**, only one helical chain was directed by Cd(II) ions and L_3 ligands(Scheme 1).

Taking the coordinated sites of backbones for organic ligands, the influence of dicarboxylates on the nets is also revealed by the structural differences. For example, Complex {[Cd(1,4-BDC)(IP)(H_2O)]·0.5H_2O}(1,4-H_2BDC = 1,4-benzendicarboxylic acid) has a 1D undulating structure with [Cd(1,4-BDC)(IP)] as its repeating unit[20]. When an additional coordinative site was introduced into the benzene ring, a higher dimension of compound **1** was obtained herein. This result indicates that the coordinative backbones can manipulate the nuclear numbers and final resulting structures. This phenomenon is also observed in flexible organic carboxylate and Cd-IP system [20].

5.5. TGA and photoluminescence properties

The decomposition behaviors of **1–3** were examined *via* thermogravimetric analysis (TGA) (Fig. S1). For **1,** first weight loss of 4.9% is detected over the range 35–190 °C, corresponding to the loss of the coordinated water molecules (calcd. 5.2%). The polycrystalline sample is stable up to 405 °C which the decomposition starts. For **2**, the TGA reveals there is a weight loss (found: 7.53%) from ca. 45 to 320 °C, corresponding to the loss of the free CH_3OH and DMF molecules (calcd: 7.1%). For **3**, the TGA reveals the polycrystalline sample is stable up to 298 °C above which the decomposition starts.

In order to confirm the phase of the bulk materials, X-ray powder diffraction (XRPD) experiments were carried out on compounds **1**–**3** (Fig. S2). The XRPD experimental and computer-simulated patterns of all them are shown in Fig. S2. Although the experimental patterns have a few unindexed diffraction lines and some slightly broadened in comparison with those simulated

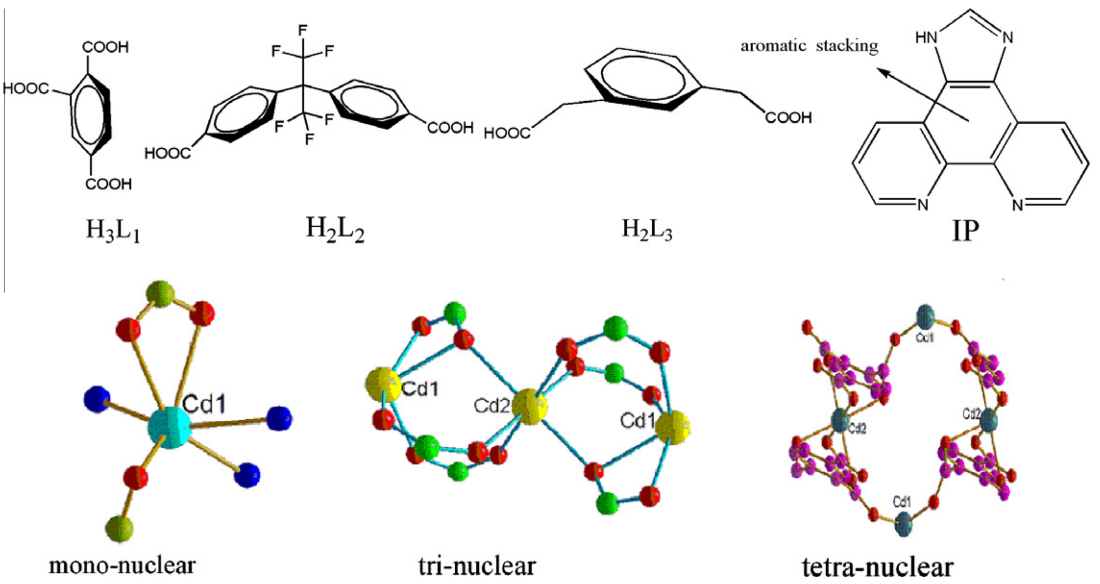

Scheme 1. Schematic representation of the ligands and nuclear number.

patterns, it can also be considered that the as-synthesized materials are homogeneous. For compound **1**, after heating at 200 °C for 5 h, the coordinative water molecules were removed (the evacuated framework is defined as **1'**). The XRPD pattern of **1'** is similar to compound **1**, although minor differences can be seen in the positions, intensities, and widths of some peaks, which indicates that the framework of compound **1** is retained after the removal of the coordinative water molecules.

Organic–inorganic coordination polymers, especially those with d^{10} metal centers, have been investigated for their fluorescent properties and potential applications as fluorescent-emitting materials, such as light-emitting diodes(LEDs)[24–25]. Therefore, the complexes **1**–**3** were studied in the solid-state at room temperature. Excitation of the microcrystalline samples at 350 nm leads to the generation of fluorescent emissions (Fig. 4), with the peak maxima occurring at 501 nm for **1**, 458 nm for **2**, 514 nm for **3**. The fluorescent spectrum of IP has been also measured, which behaves a relatively broad band at 460 nm (λ_{ex} = 315 nm)[20]. The emission bands of these carboxylates can be assigned to the $\pi* \rightarrow n$ transition as previously reported. The fluorescent emission of the carboxylate ligands deriving from the $\pi* \rightarrow n$ transition is very weaker than those of the $\pi* \rightarrow \pi$ transition n of the IP ligand, thus, the carboxylate ligands almost have no contribution to the fluorescent emission of the complexes. For the emission bands of **1**–**3** are located in red-shift positions, which may be assigned to the $\pi* \rightarrow \pi$ transitions, whereas the significant redshifts of these bands in comparison to that of IP would be attributed to the metal–ligand coordinative behaviors and their different conjugated structures.

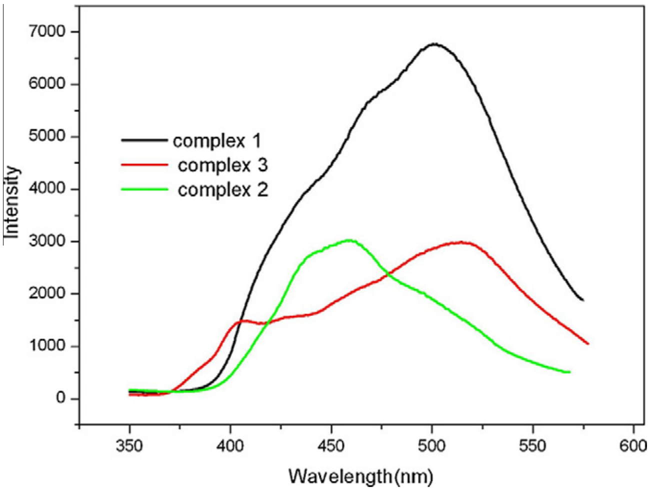

Fig. 4. Solid-state emission spectra of compounds **1**–**3** at room temperature.

6. Conclusion

In summary, the simultaneous use of carboxylate ligands and the pharmaceutical agent IP ligand reacting with Cd(II) ions affords three new polymers. Although the polymers possess 2D structural motifs, the tridentate mode of IP ligand is only observed in complex **3**. All the complexes have high stabilities and intense fluorescent emissions. This work shows that tuning the backbone of organic ligand is an effective strategy in crystal engineering of preparing metal–organic frameworks.

Acknowledgment

We gratefully acknowledge financial support of this work by the Guangdong Medical College.

Appendix A. Supplementary material

Crystallographic data for the structural analysis have been deposited with the Cambridge Crystallographic Data Centre, CCDC No. 768703–768705 for compounds **1**–**3**. Copies of this information may be obtained free of charge on application to CCDC, 12 Union Road, Cambridge CB2 1EZ, UK (fax: +44 1223 336 033; e-mail: deposit@ccdc.cam.ac.uk or http://www.ccdc.cam.ac.uk).

Supplementary data associated with this article can be found, in the online version, at doi:10.1016/j.molstruc.2010.12.006.

References

[1] (a) O.M. Yaghi, J.L.C. Rowsell, J. Am. Chem. Soc. 128 (2006) 1304;
(b) X. Zhao, B. Xiao, A.J. Fletcher, K.M. Thomas, D. Bradshaw, M.J. Rosseinsky, Science. 306 (2004) 1012;
(c) N.L. Rosi, J. Eckert, M. Eddaoudi, D.T. Vodak, J. Kim, M. O'. Keeffe, O.M. Yaghi, Science. 300 (2003) 1127.
[2] Y.W. Li, R.T. Yang, J. Am. Chem. Soc. 128 (2006) 726.

[3] Y. Kubota, M. Takata, R. Matsuda, R. Kitaura, S. Kitagawa, K. Kato, M. Sakata, T.C. Kobayashi, Angew. Chem., Int. Ed. 44 (2005) 920.
[4] (a) F.Y. Lian, F.L. Jiang, D.Q. Yuan, J.T. Chen, M.Y. Wu, M.C. Hong, Cryst Eng Comm 10 (2008) 905;
(b) R. Mondal, M.K. Bgunia, K. Dhara, Cryst Eng Comm 10 (2008) 1167.
[5] X.-M. Zhang, M.-L. Tong, M.-L. Gong, X.-M. Chen, Eur. J. Inorg. Chem. (2003) 138.
[6] L.-M. Duan, F.-T. Xie, X.-Y. Chen, Y. Chen, Y.-K. Lu, P. Cheng, J.-Q. Xu, Cryst. Growth & Des. 6 (2006) 1101.
[7] A. Beghidja, P. Rabu, G. Rogez, R. Welter, Chem. Eur. J. 12 (2006) 7627.
[8] M.-L. Tong, H.–K. Lee, Y.–X. Tong, X.–M. Chen, T.C.W. Mak, Inorg. Chem. 39 (2000) 4666.
[9] R.P. Davies, R.J. Less, P.D. Lickiss, A.J.P. White, Dalton Trans. (2007) 2528.
[10] Y. Wei, H.W. Hou, L.K. Li, Y.T. Fan, Y. Zhu, Cryst. Growth Des. 5 (2005) 1405.
[11] G.B. Che, C.B. Liu, B. Liu, Q.W. Wang, Z.L. Xu, Cryst Eng Comm 10 (2008) 184.
[12] T.L. Hu, R.Q. Zou, J.R. Li, X.H. Bu, Dalton Trans. (2008) 1302.
[13] Z.-H. Zhou, G.-F. Wang, S.-Y. Hou, H.-L. Wan, K.-R. Tsai, Inorg. Chim. Acta. 314 (2001) 184.
[14] D.R. Xiao, E.B. Wang, H.Y. An, Y.G. Li, Z.M. Su, C.Y. Sun, Chem. Eur. J. 12 (2006) 6528.
[15] X.L. Wang, C. Qin, E.B. Wang, Z. M. Su 12 (2006) 2680.
[16] Y. Xiong, X.-F. He, X.-H. Zou, J.-Z. Wu, X.-M. Chen, L-N. Ji, R.-H. Li, J.-Y. Zhou, K.-B. Yu, J. Chem.Soc., Dalton Trans. (1999) 19.
[17] B. Zhao, P. Cheng, Y. Dai, C. Cheng, D.Z. Liao, S.P. Yan, Z.H. Jiang, G.L. Wang, Angew. Chem., Int. Ed. 42 (2003) 943.
[18] M.D. Stephenson, T.J. Prior, M.J. Hardie, Cryst. Growth Des. 8 (2008) 643.
[19] X.L. Wang, H.Y. Lin, T.L. Hu, J.L. Tian, X.H. Bu, J. Mol. Struct 798 (2006) 34.
[20] J.Q. Liu, Y.N. Zhang, Y.Y. Wang, J.C. Jin, E.L. Lermontova, Q.Z. Shi, Dalton Trans. (2009) 5365.
[21] G. M. Sheldrick, SHELXL-97; University of Göttingen: Germany, 1997.
[22] G.M. Sheldrick, SADABS 2.05; University of Göttingen: Germany, 2002.
[23] J. Tao, M.L. Tong, J. Shi, X.M. Chen, Wen. Ng, S. Chem. Commun. (2000) 2043.
[24] X. Ouyang, D. Liu, T. Okamura, H. Bu, W. Sun, W. Tang, N. Ueyanma, Dalton Trans. (2003) 1836.
[25] K. Balasubramanian, RelatiVistic Effects in Chemistry* Part A: Theory and Techniques; Part B: Applications, Wiley, New York, 1997.